

# A synthesis of fluid and thermal transport models for metal foam heat exchangers

Shadi Mahjoob, Kambiz Vafai\*

*Mechanical Engineering Department, University of California, Riverside, CA 92521, USA*

Received 24 October 2007; received in revised form 16 December 2007

Available online 28 March 2008

## Abstract

Metal foam heat exchangers have considerable advantages in thermal management and heat recovery over several commercially available heat exchangers. In this work, the effects of micro structural metal foam properties, such as porosity, pore and fiber diameters, tortuosity, pore density, and relative density, on the heat exchanger performance are discussed. The pertinent correlations in the literature for flow and thermal transport in metal foam heat exchangers are categorized and investigated. Three main categories are synthesized. In the first category, the correlations for pressure drop and heat transfer coefficient based on the microstructural properties of the metal foam are given. In the second category, the correlations are specialized for metal foam tube heat exchangers. In the third category, correlations are specialized for metal foam channel heat exchangers. To investigate the performance of the foam filled heat exchangers in comparison with the plain ones, the required pumping power to overcome the pressure drop and heat transfer rate of foam filled and plain heat exchangers are studied and compared. A performance factor is introduced which includes the effects of both heat transfer rate and pressure drop after inclusion of the metal foam. The results indicate that the performance will be improved substantially when a metal foam is inserted in the tube/channel.

© 2008 Elsevier Ltd. All rights reserved.

## 1. Introduction

Metal foams are a class of porous materials with low densities and novel thermal, mechanical, electrical and acoustic properties [1]. The foams are lightweight, offering high strength and rigidity, nontoxic structure, high surface area and recyclable which improve energy absorption and heat transfer in thermal applications, such as heat exchangers. The rate of heat transfer is enhanced by conducting the heat to the material struts, which have a large accessible surface area per unit volume, along with high interaction with the fluid flowing through them [2–7]. Normal foam ligaments in the flow direction results in boundary layer disruption and mixing. Turbulence and unsteady flow occur for pore-scale Reynolds number greater than 100 [8]. The effect of thermal dispersion is essential for a number of applications in the transport processes. Vafai et al. have shown that

the effect of transverse dispersion is much more important than the longitudinal dispersion [9,10]. The induced turbulence and dispersion cause further enhancement in heat transfer and increase performance and efficiency of the heat exchanger considerably [11,12]. In addition, flow paths through the foam are interconnected, which makes the flow available in all areas. As such, utilizing the metal foam leads to smaller and lighter heat exchangers.

Metal foams have considerable applications in multifunctional heat exchangers [13–17], cryogenics [18], combustion chambers, cladding on buildings, strain isolation, buffer between a stiff structure and a fluctuating temperature field, geothermal operations, petroleum reservoirs, compact heat exchangers for airborne equipments, air-cooled condenser towers and cooling systems [19], high power batteries [20], compact heat sinks for power electronics and electronic cooling [17,21–24], heat pipes [25,26] and sound absorbers [27–30].

Metal foams can be classified as porous media with typically high porosity that consists of tortuous, irregular

\* Corresponding author. Tel.: +1 951 827 2135; fax: +1 951 827 2899.  
E-mail address: [vafai@engr.ucr.edu](mailto:vafai@engr.ucr.edu) (K. Vafai).

## Nomenclature

$a_{sf}$	specific surface area	$R_2$	radius of the outer side of the outer tube
$Bi$	Biot number	$Re$	Reynolds number
$c_p$	specific heat at constant pressure	$S_{fs}$	fluid solid interface in CRUC
$C_D$	form drag coefficient	$S_v$	surface area per unit volume of solid phase
CRUC	cubic representative unit cell	$u$	velocity
$d$	width of CRUC	$U$	overall heat transfer coefficient
$d_f$	metal foam fiber diameter	$V_0$	total volume of CRUC
$d_p$	mean pore diameter	$x$	longitudinal coordinate
$D_p$	the equivalent spherical diameter of a porous medium	$y$	transverse coordinate
$D_h$	hydraulic diameter of channel	$Y$	nondimensional transverse coordinate
$Da$	Darcy number		
$f$	friction factor	<i>Greek symbols</i>	
$F$	inertial coefficient	$\varepsilon$	porosity
$G$	shape function	$\kappa$	ratio of fluid to solid effective thermal conductivity
$h$	heat transfer coefficient	$\rho$	density
$h_{sf}$	interfacial heat transfer coefficient	$\mu$	dynamic viscosity
$H$	the height of the foam channel	$\nu$	kinematic viscosity
$j^*$	modified Colburn $j$ -factor	$\chi$	tortuosity
$k$	thermal conductivity	$\eta$	pump efficiency
$K$	permeability	$\theta_{r,b}$	dimensionless bulk mean fluid temperature
$L$	length of the foam channel		
$Nu$	overall Nusselt number	<i>Subscripts</i>	
$Nu_{sf}$	interfacial overall Nusselt number	b	bulk
$P$	dimensionless pressure	e	effective
$P_{p,\eta}$	pumping power	f	fluid
$Pr$	Prandtl number	i	inner tube
$q$	heat flux	o	outer tube
$R$	radius of the inner tube	s	solid
$R_1$	radius of the inner side of the outer tube	w	wall

shaped flow passages. However, some aspects of the past studies on packed beds and granular porous media needs to be modified for metal foams [18]. Liu et al. [31] have indicated that the pressure drop resulting from foam matrices, is much lower than that by granular matrices at the same Reynolds number. Metal foams include small filaments that are continuously connected in an open-celled foam structure. Metal foam cells are usually polyhedrons of 12–14 faces in which each face has a pentagonal or hexagonal shape (by five or six filaments). Due to the geometric complexity and the random orientation of the solid phase of the porous medium, the solution of the transport equations inside the pores is difficult to obtain. As such, the foam cell geometric idealizations (such as cubic unit cell model) has been employed for analytical and computational studies which can be inaccurate especially for compressed metal foam modeling [32]. In an effort to simulate flow through foam filaments computationally, Boomsma et al. [33] modeled idealized open-cell metal foams based on a fundamental periodic unit of eight cells. Fluid flow was then modeled computationally utilizing a

three-dimensional cellular unit along with periodic boundary conditions.

The strength of the foam depends mainly on the base material and the relative density of the foam. Other properties, such as pore size, pore density, area density, fiber size, and cell shape affect certain foam characteristics, such as pressure drop and heat transfer [34,35]. Pore size and relative density affect the foam's flexibility [8]. The pore size is specified by the diameter of the open space in each of the cell faces. Typically this open space varies between 0.3 mm and 4 mm [1]. The pore density is the number of pores per unit length of the material specified as PPI (pores per inch). The available pore densities vary based on the foam material. However, the typical overall uncompressed range is 5–100 PPI. The relative density is the volume of solid foam material relative to the total volume of metal foam. As such, an increase in the relative density improves the strength of the foam structure, since the filaments become larger in diameter and stronger. The area density is the ratio of the surface area of the foam to its volume.

Due to the high thermal conductivity and structural strength of aluminum, the open-cell aluminum foams have attracted the attention of researchers for heat exchanger design. The porosity of a foam metal can be estimated using the weight of a given volume of the sample and the density of the metal. The average fiber diameter,  $d_f$ , can be measured using a microscope, and the average pore diameter,  $d_p$ , can be estimated by counting the number of pores in a given length of material. The pore density (PPI) is a nominal value supplied by the manufacturer [36].

Du Plessis et al. [37] established models for pore diameter estimation as a function of tortuosity, porosity, total volume and fluid–solid interface area of a cubic representative unit cell (CRUC), a foam cell geometric approximation, and also represented as a function of the width of the cubic representative unit cell ( $d = d_p + d_f$ ) (Table 1, Eq. (1)). Other models by Du Plessis et al. [37,38] for pore and fiber diameters are presented as functions of porosity, tortuosity, and the width of the cubic representative unit cell (Table 1, Eqs. (2)–(4)). Also, Calmidi [39] developed a model for the fiber diameter estimation as a function of porosity, pore diameter and shape function for a cubic unit cell (Table 1, Eq. (5)). Calmidi [39] also presented a modified model utilizing three-dimensional dodecahedron unit cell structure (Table 1, Eq. (6)). The authors showed that this model has a maximum deviation of  $\pm 7\%$  from measured values for pore and fiber diameters. Experimental investigation of Bhattacharya et al. [40] indicates that the tortuosity model by Du Plessis et al. [37] (Table 2, Eq. (1)) is accurate mainly for high pore densities. Bhattacharya et al. [40] established a model for tortuosity as a function of porosity and shape function ( $G$ ), which can cover a wider range of pore densities and porosities [40] (Table 2, Eq. (2)). The shape function includes the fiber cross section variation with porosity.

An open-cell metal foam filled pipe is investigated by Lu et al. [41]. The results show that the overall Nusselt number of the pipe increases with an increase in the relative density or pore density (PPI), especially when the thermal conductivity of the solid is much higher than that of the fluid.

Although metal foams with low porosity and small pore size (i.e. high pore density) are preferred for achieving high heat transfer performance, they lead to a significant increase in the pressure drop. However, larger pore size materials can also lead to larger Nusselt numbers at higher flow rates with relatively lower pumping power [12,13]. Lu et al. [41] demonstrated that for low Reynolds numbers, the effects of the thermal conductivity of the foam on heat transfer is quite small. Therefore, cheaper and lower thermal conductivity foams can be used at lower flow rates. When low thermal conductivity foams are utilized, the effect of pore density would be quite small. As such, higher porosity foams can be employed for these cases resulting in lower pressure drops. Compared to plain tubes, metal foam filled tubes have significantly higher (up to 40 times) heat transfer performance [41].

Klett et al. [42] indicated that solid foam radiators can transfer heat an order of magnitude better than the fin radiators. Boomsma et al. [18] indicated that the thermal resistances generated by the compressed open-cell aluminum foam heat exchangers were two to three times lower than the commercially available heat exchangers, while requiring about the same pumping power. Bhattacharya and Mahajan [24] studied the finned metal foam heat sinks for electronic cooling in which the air gap between two adjacent longitudinal fin heat sinks was replaced by high porosity metal foams. The results display that the heat transfer was enhanced by a factor of 1.5–2. Kim et al. [43,44] examined heat transfer through aluminum foams inserted between two isothermal plates. Their results show that the foam material have better heat transfer performance compared to the conventional array fins, but subject to a greater pressure drop. As such, metal foam heat exchangers provide a significant improvement over the commercially available heat exchangers, which operate under similar conditions.

Modeling or measurement techniques have been developed for effective thermal conductivities of solid–fluid structures [40,45–54]. Dukhan and Quinones [55] have stated that the effective thermal conductivity of the aluminum

Table 1  
A synthesis of pertinent correlations for metal foam pore and fiber diameters

References	Correlation <sup>a</sup>	Equation Nos.
Du Plessis et al. [37]	$d_p = \frac{6\varepsilon}{\chi}(\chi - 1) \frac{V_0}{S_{fs}} = \frac{2\varepsilon \cdot d}{\chi(3 - \chi)}$	(1)
	$d_p = \sqrt{\frac{\varepsilon}{\chi}} d \quad d_f = \left(1 - \sqrt{\frac{\varepsilon}{\chi}}\right) d$	(2–3)
Fourie and Du Plessis [38]	$d_p = \frac{3 - \chi}{2} d$	(4)
Calmidi [39]	$\frac{d_f}{d_p} = 2\sqrt{\frac{(1 - \varepsilon)}{3\pi}} \frac{1}{G} = 2\sqrt{\frac{(1 - \varepsilon)}{3\pi}} \frac{1}{1 - e^{-(1 - \varepsilon)/0.04}}$	(5)
	$\frac{d_f}{d_p} = 1.18\sqrt{\frac{(1 - \varepsilon)}{3\pi}} \frac{1}{G} = 1.18\sqrt{\frac{(1 - \varepsilon)}{3\pi}} \frac{1}{1 - e^{-(1 - \varepsilon)/0.04}}$	(6)

<sup>a</sup> Expressions for  $\chi$  are given in Table 2.

Table 2  
A synthesis of pertinent correlations for metal foam tortuosity and specific surface area

References	Correlation	Equation Nos.
Du Plessis et al. [37]	$\frac{1}{\chi} = \frac{3}{4\varepsilon} + \frac{\sqrt{9-8\varepsilon}}{2\varepsilon} \times \cos \left\{ \frac{4\pi}{3} + \frac{1}{3} \cos^{-1} \left[ \frac{8\varepsilon^2 - 36\varepsilon + 27}{(9-8\varepsilon)^{3/2}} \right] \right\}$	(1)
Bhattacharya et al. [40]	$\frac{1}{\chi} = \frac{\pi}{4\varepsilon} \left\{ 1 - \left( 1.18 \sqrt{\frac{(1-\varepsilon)}{3\pi}} \frac{1}{G} \right)^2 \right\} = \frac{\pi}{4\varepsilon} \left\{ 1 - \left( 1.18 \sqrt{\frac{(1-\varepsilon)}{3\pi}} \frac{1}{1 - e^{-(1-\varepsilon)/0.04}} \right)^2 \right\}$	(2)
Calmidi and Mahajan [36]	$a_{sf} = \frac{3\pi d_f}{(0.59d_p)^2} [1 - e^{-((1-\varepsilon)/0.04)}]$	(3)
Fourie and Du Plessis [38]	$a_{sf} = \frac{3}{d} (3 - \chi)(\chi - 1)$	(4)

foams can be up to four times larger than that of the solid aluminum thus substantially improving the heat transfer. Boomsma and Poulikakos [54] have established a correlation for the effective thermal conductivity. Their studies indicate that changing the fluid conductivity has a relatively small effect on increasing the effective thermal conductivity. As such, the thermal conductivity of the solid phase and porosity have the main effect on the overall effective thermal conductivity.

Calmidi and Mahajan [36] studied the solid-to-fluid heat transfer from a heated metal channel brazed to an aluminum metal foam. Their results indicate that thermal dispersion is quite low when air is passing through the metal foam. However, dispersion would be considerably larger in the case of water, as it was previously represented by Hunt and Tien [4]. The dispersion conductivity is usually dominant at high Reynolds numbers, especially if the effective thermal conductivity is low [36]. Phanikumar and Mahajan [56] investigated buoyancy driven flow through metal foams. Their results indicate that at high Rayleigh and Darcy numbers, the fluid and foam fiber temperature difference would be significant requiring the utilization of a local thermal nonequilibrium model (LTNE).

The assumption of local thermal equilibrium (LTE) has widely been used in analyzing transport processes through porous media. However, this assumption is not valid for applications where a substantial temperature difference exists between the solid phase and the fluid phase [57]. Amiri and Vafai [3,58] employed the generalized model for the momentum equation and a two-phase model for the energy equation, including axial and transverse thermal dispersion to investigate forced convection and validated their findings utilizing experimental investigations. They presented detailed error maps for assessing the importance of various simplifying assumptions that are commonly used. In addition, they presented a comprehensive analysis of transient incompressible flow including inertia and boundary effects and the effects of thermal dispersion and local thermal nonequilibrium (LTNE) in the energy equation [59]. Alazmi and Vafai [60] comprehensively investigated the proper form of boundary conditions for constant wall heat flux in porous media under LTNE con-

ditions. Effects of variable porosity and thermal dispersion were also analyzed. Lee and Vafai [61] classified the heat transfer characteristics through porous media within three regimes, each of which is dominated by one of three distinctive heat transfer mechanisms: fluid conduction, solid conduction and internal heat exchange between solid and fluid phases and presented pertinent analytical expressions for each regime. Marafie and Vafai [57] investigated analytically forced convection through a channel filled with a porous medium, utilizing Darcy–Forchheimer–Brinkman model and local thermal nonequilibrium energy transport model. Analytical solutions were obtained for both fluid and solid temperature fields incorporating the effects of various pertinent parameters such as Biot number, the thermal conductivity ratio, Darcy number and inertial parameters.

## 2. Pressure drop and heat transfer correlations for metal foam heat exchangers

Pressure drop and heat transfer coefficient are the two important factors to be considered in designing a heat exchanger. The available correlations in the literature for metal foam heat exchangers can be classified in terms of three pertinent categories. In the first category, the correlations are independent of heat exchanger geometry and function of microstructure of the foam. In this category the friction factor and pressure drop can be estimated directly through the correlations or through the Ergun equation utilizing the pertinent correlations for permeability and inertial coefficient for metal foams. In the second category, the correlations are developed for the foam filled tube heat exchangers. Based on the correlations within this category, a tube heat exchanger can be designed for applications where the inner tube, the outer tube or both are filled with foam metals. The third category relates to metal foam channel heat exchangers filled with foam metals.

In what follows, these three categories are discussed in more detail. The results given for these categories are based on thermally and hydraulically fully developed flow. Furthermore, all thermodynamic properties of the solid

and fluid are considered to be temperature independent and natural convection and radiation are assumed to be negligible and the porous medium is assumed homogenous and isentropic. A synthesis of pertinent correlations for metal foam pore and fiber diameters is presented in Table 1. A synthesis of pertinent correlations for metal foam tortuosity and specific surface area is presented in Table 2 and a synthesis of fluid and thermal transport models of metal foam heat exchangers is given in Table 3.

### 2.1. Category I: Microstructural based correlations for metal foam heat exchangers

Paek et al. [47] and Liu et al. [31] have established friction factor models to predict the pressure drop. In the empirical model by Paek et al. [47], friction factor is a function of pore Reynolds number (Table 3, Eq. (1)). Liu et al. [31] presented empirical correlations for the friction factor of airflow through aluminum metal foam with different porosities at different fluid regimes (Table 3, Eqs. (2)–(4)). Pressure drop can be estimated through Ergun relationship established for granular porous material (Table 3, Eq. (5)) [62].

The other cited models for pressure drop prediction are mainly permeability and inertial coefficient correlations for Forchheimer extended Darcy's equation for homogenous and isotropic porous media given as:

$$-\frac{dP}{dx} = \frac{\mu}{K}u + \frac{\rho F}{\sqrt{K}}u^2$$

One of the systematic evaluations of permeability and inertia coefficient of metal foams is done by Vafai and Tien [7] utilizing experimental and theoretical investigations. They reported values of  $1.11 \times 10^{-7} \text{ m}^2$  and 0.057 for permeability and inertia coefficient, respectively in a manner similar to those experimentally reported later [3]. Du Plessis et al. [37] established a theoretical model for prediction of inertial coefficient and permeability utilizing a cubic representative unit cell (CRUC) concept, along with experimental measurements. The CRUC resembles three-dimensional fluid flow around a metallic wire. The correlations are functions of porosity, average pore diameter, and tortuosity (Table 3, Eqs. (6) and (7)). The width of the cubic representative unit cell ( $d$ ) can be calculated from Eq. (2) (Table 1). In an experimental and analytical work by Calmidi [39], inertial parameter and permeability were modeled as functions of average pore and fiber diameters and porosity (Table 3, Eqs. (8) and (9)). As it was mentioned earlier, the author developed a model for  $d_f/d_p$  as a function of porosity (Table 1, Eqs. (5) and (6)).

In an experimental and analytical work, Bhattacharya et al. [40] established a correlation for the inertial coefficient as a function of porosity, tortuosity, shape factor and form drag coefficient (Table 3, Eqs. (10)–(13)). For permeability, they used the model proposed by Du Plessis et al. [37]. The theory of flow over bluff bodies was employed to predict the inertial coefficient. Dukhan [32]

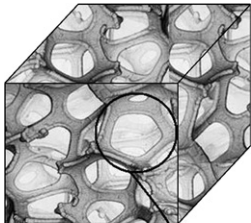
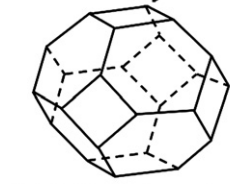
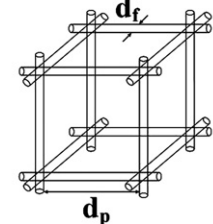
established empirical correlations for permeability and inertial coefficient as a function of porosity (Table 3, Eqs. (14) and (15)). In their model, permeability had an exponential dependence on porosity. This behavior was also observed in presented data of Antohe et al. [63] in which hydraulic characterization of compressed aluminum foams were investigated experimentally. Tadriss et al. [64] established an empirical model for inertial coefficient and permeability estimation based on Ergun relationship as functions of porosity and fiber diameter (Table 3, Eqs. (16) and (17)). A theoretical model is established for inertial coefficient by Fourie and Du Plessis [38] utilizing an ordered array of tetrakaidecahedra geometric idealization (Table 3, Eqs. (18) and (19)). The inertial coefficient is a function of porosity, tortuosity and form drag coefficient ( $C_D$ ) which depends on the Reynolds number. For permeability, they suggested the model proposed by Du Plessis et al. [37].

For heat transfer calculations, Calmidi and Mahajan [36] and Shih et al. [65] developed correlations for interfacial heat transfer parameters and pore diameter Nusselt numbers. In experimental and numerical works by Calmidi and Mahajan [36], correlations for the specific solid–fluid interfacial surface area, interfacial Nusselt number and heat transfer coefficient were established as a function of fiber and pore diameter and porosity (Table 2, Eq. (3) and Table 3, Eq. (20)). In their numerical simulation, a semi-empirical volume averaged form of the governing equations was utilized invoking local thermal nonequilibrium technique. The interfacial terms couple the solid and fluid phase thermal nonequilibrium energy equations. The interfacial heat transfer models [36] are based on a correlation by Zukauskas [66] for cylinders in cross-flow in the range of Reynolds numbers (40–1000). Zukauskas's models were also employed by Lu et al. [41], Zhao et al. [67], and Phanikumar and Mahajan [56] for interfacial heat transfer coefficient prediction. Since the temperature gradients in radial direction within the fibers are expected to be small, utilization of the Nusselt number correlation for external flow over a body of an appropriate cross section appears to be a reasonable approximation. The coefficient ( $C_T$ ) was confirmed by matching the experimental and numerical data [36]. The specific solid–fluid interfacial surface area ( $a_{sf}$ ) was developed for arrays of parallel cylinders employed in three mutually perpendicular directions utilizing dodecahedra unit cell geometric modeling (Table 2, Eq. (3)). Another model for specific surface area ( $a_{sf}$ ) was established by Fourie and Du Plessis [38] based on the cubic representative unit cell (CRUC) (Table 2, Eq. (4)). In an experimental investigation by Shih et al. [65], pore diameter Nusselt number is established as a function of pore diameter and porosity (Table 3, Eq. (21)).

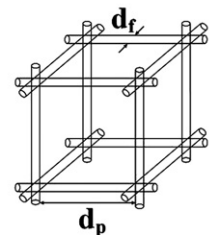
### 2.2. Category II: Metal foam tube heat exchangers

In an analytical investigation by Lu et al. [41,67], a metal foam tube heat exchanger is modeled and pertinent correlations for friction factor, pressure drop and heat transfer

Table 3  
A synthesis of fluid and thermal transport models of metal foam heat exchangers

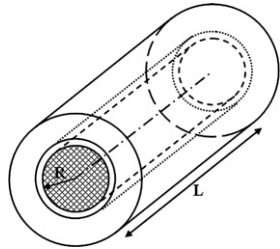
Category	References	Correlation	Equation Nos.
Category I: Microstructural based correlations for metal foam heat exchangers	Paek et al. [47]	$\frac{(\Delta P/L)\sqrt{K}}{\rho u^2} = f = \frac{1}{Re_K} + 0.105 = \frac{\mu}{\rho u \sqrt{K}} + 0.105$	(1)
	Liu et al. [31]	For $30 < Re_{dp} < 300$ : $f = 22 \frac{1-\varepsilon}{Re_{dp}} + 0.22$ For $Re_{dp} \gg 300$ : $f = 0.22$	(2–3)
		$Re_{dp} = \frac{D_p \rho u}{\mu} (1-\varepsilon) = \frac{6\rho u}{\mu S_v} (1-\varepsilon) = \frac{3\rho u d_p}{2\mu\varepsilon} (1-\varepsilon)^2$ $\frac{\Delta P}{L} = f \frac{\rho u^2}{D_p} \frac{1-\varepsilon}{\varepsilon^3}$	(4–5)
	Du Plessis et al. [37]	$\frac{K}{d^2} = \frac{\varepsilon^2}{36\chi(\chi-1)}$ $F = \frac{2.05\chi(\chi-1)\sqrt{K}}{\varepsilon^2(3-\chi)d}$	(6–7)
	Calmidi [39]	$\frac{K}{d_p^2} = 0.00073(1-\varepsilon)^{-0.224} \left(\frac{d_f}{d_p}\right)^{-1.11}$ $F = 0.00212(1-\varepsilon)^{-0.132} \left(\frac{d_f}{d_p}\right)^{-1.63}$	(8–9)
	Bhattacharya et al. [40]	$F = 0.095 \frac{C_{D(\varepsilon=0.85)}}{12} G^{-0.8} \sqrt{\frac{\varepsilon}{3(\chi-1)}} \left(1.18 \sqrt{\frac{(1-\varepsilon)}{3\pi} \frac{1}{G}}\right)^{-1}$ $C_{D(\varepsilon=0.85)} = 1.2$	(10–11)
		For $0.85 < \varepsilon < 0.97$ : $G = 1 - e^{-(1-\varepsilon)/0.04}$ For $\varepsilon \geq 0.97$ : $G = 0.5831$	(12–13)
	Dukhan [32]	$K = a_1 \exp[b_1 \varepsilon]$ $F = (a_2 \varepsilon + b_2) \sqrt{K}$ $a_1, a_2, b_1$ and $b_2$ are constants.	(14–15)
	Tadrist et al. [64]	$K = \frac{\varepsilon^3 d_f^2}{\alpha(1-\varepsilon)^2}$ $\frac{F}{\sqrt{K}} = \frac{\beta(1-\varepsilon)}{\varepsilon^3 d_f}$ $\alpha : 100 - 865$ , $\beta : 0.65 - 2.6$	(16–17)
	Fourie and Du Plessis [38]	$F = (3-\chi)(\chi-1) \frac{C_D \chi^{1.5}}{24\varepsilon^3}$ $C_D = 1 + (10/Re)^{0.667} = 1 + 10(\rho u d_f (\chi-1)/2\mu\varepsilon)^{-0.667}$	(18–19)
	Calmidi and Mahajan [36]	$Nu_{sf} = \frac{h_s d_f}{k_f} = C_T Re_{d_f}^{0.5} Pr^{0.37} = C_T \left(\frac{u d_f}{\nu}\right)^{0.5} Pr^{0.37}$ ( $C_T = 0.52$ )	(20)
	Shih et al. [65]	$Nu_{Dp} = \frac{h D_p}{k_{se}} = a Re_{Dp}^b = a \left(\frac{\rho u D_p}{\mu}\right)^b$ $a$ and $b$ are constants.	(21)

Tetraprismatic unit cell model



Cubic unit cell model

Category II: Metal foam tube heat exchangers



Lu et al. [41]

$$f = \frac{4\mu}{K\rho u} PR = \frac{8P}{Da \cdot Re} \quad \frac{\Delta P}{L} = \frac{\mu}{K} uP \quad P = \frac{J_0\left(\sqrt{\frac{\varepsilon}{Da}}\right)}{2\sqrt{\frac{Da}{\varepsilon}} J_1\left(\sqrt{\frac{\varepsilon}{Da}}\right) - J_0\left(\sqrt{\frac{\varepsilon}{Da}}\right)} \quad (22-24)$$

$$Nu_i = \frac{h_i}{k_f} 2R = \frac{2Rq_w}{k_f(T_w - T_{f,bi})} = -\frac{2k_{sc}}{k_f\theta_{f,bi}} \quad Da = \frac{K}{R^2} \quad (25-26)$$

where,  $J_0$  and  $J_1$  are Bessel functions. These correlations are developed for the foam filled inner tube of the heat exchanger.

Zhao et al. [67]

$$\frac{\Delta P}{L} = \frac{\mu}{K} uP \quad (27)$$

$$P = \frac{(R_2/R_1)^2 - 1}{2\sqrt{\frac{Da}{\varepsilon}} \left( N_1 \left( \frac{R_2}{R_1} \cdot J_1\left(\sqrt{\frac{\varepsilon}{Da}} \frac{R_2}{R_1}\right) - J_1\left(\sqrt{\frac{\varepsilon}{Da}}\right) \right) + N_2 \left( \frac{R_2}{R_1} \cdot Y_1\left(\sqrt{\frac{\varepsilon}{Da}} \frac{R_2}{R_1}\right) - Y_1\left(\sqrt{\frac{\varepsilon}{Da}}\right) \right) \right) - \left( \frac{R_2}{R_1} \right)^2 + 1} \quad (28)$$

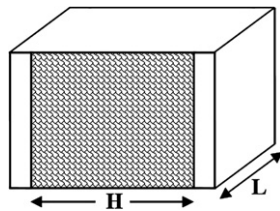
$$N_1 = \frac{Y_0\left(\sqrt{\frac{\varepsilon}{Da}}\right) - Y_0\left(\sqrt{\frac{\varepsilon}{Da}} \frac{R_2}{R_1}\right)}{J_0\left(\sqrt{\frac{\varepsilon}{Da}} \frac{R_2}{R_1}\right) \cdot Y_0\left(\sqrt{\frac{\varepsilon}{Da}}\right) - Y_0\left(\sqrt{\frac{\varepsilon}{Da}} \frac{R_2}{R_1}\right) \cdot J_0\left(\sqrt{\frac{\varepsilon}{Da}}\right)} \quad (29)$$

$$N_2 = \frac{J_0\left(\sqrt{\frac{\varepsilon}{Da}}\right) - J_0\left(\sqrt{\frac{\varepsilon}{Da}} \frac{R_2}{R_1}\right)}{Y_0\left(\sqrt{\frac{\varepsilon}{Da}} \frac{R_2}{R_1}\right) \cdot J_0\left(\sqrt{\frac{\varepsilon}{Da}}\right) - J_0\left(\sqrt{\frac{\varepsilon}{Da}} \frac{R_2}{R_1}\right) \cdot Y_0\left(\sqrt{\frac{\varepsilon}{Da}}\right)} \quad (30)$$

$$Nu_o = \frac{2h_o}{k_f} (R_2 - R_1) = \frac{2q_w(R_2 - R_1)}{k_f(T_w - T_{f,bo})} = -\frac{k_{sc}}{k_f\theta_{f,bo}} \frac{2(R_2 - R_1)}{R_1} \quad Da = \frac{K}{R_1^2} \quad (31-32)$$

where,  $J_0$ ,  $J_1$ ,  $Y_0$  and  $Y_1$  are Bessel functions. These correlations are developed for the foam filled outer tube of the heat exchanger.

Category III: Metal foam channel heat exchangers



Kim et al. [43]

$$\frac{(\Delta P/L)H}{\rho u^2} = f = \frac{1}{Re_H \cdot Da} + \frac{0.105}{Da^{1/2}} \quad Re_H = \frac{uH}{\nu} \quad Da = \frac{K}{H^2} \quad (33-35)$$

$$\text{For } 270 < Re_H < 2050 \quad j^* = \frac{U}{\rho c_p u} Pr^{2/3} = 13.73(Re_H^{-0.489} Da^{0.451}) \quad (36)$$

Kim et al. [44]

$$\text{For } 1000 < Re_H < 3000 \quad Nu = 0.0159 Re_H^{0.426} Pr^{1/3} Da^{-0.787} \quad (37)$$

Lee and Vafai [61]

$$Nu = 12 \frac{1+\kappa}{\kappa} \frac{1}{1 + \frac{3}{Bi(1+\kappa)} \left\{ \left( 1 - \frac{1}{\sqrt{Bi(1+\kappa)/\kappa}} \tanh(\sqrt{Bi(1+\kappa)/\kappa}) \right) \right\}} \quad \kappa = \frac{k_{fe}}{k_{se}} \quad Bi = \frac{h_{sf} a_{sf} H^2}{4k_{se}} \quad (38-40)$$

Marafie and Vafai [57]

$$Nu = \frac{h_w D_h}{k_{fe}} = \frac{-4}{\kappa \theta_{f,b}} = \frac{-4}{\kappa \int_0^1 \left( 2 \sum_{i=1}^4 \frac{\Gamma_i(Y)}{z_i} - \frac{\mu}{2z_1} Y^2 + \frac{C_3}{z_1^3} \sinh(\alpha_1 Y) + \frac{C_4}{z_1^3} \cosh(\alpha_1 Y) + C_5 \right) dY} \quad Y = \frac{2y}{H} \quad (41-42)$$

The variables in the above equation ( $\Gamma_i$ ,  $\alpha_1$ ,  $C_3$ ,  $C_4$ ,  $C_5$ ) are specified in the reference

coefficient (overall Nusselt number) are presented (Table 3, Eqs. (22)–(32)). The Brinkman-extended Darcy model and two-equation heat transfer model for porous media were utilized to develop the correlations. The solution of dimensionless bulk mean fluid temperature for inner and outer tubes are presented by Lu et al. [41] and Zhao et al. [67]. Three different heat exchangers can be modeled with these correlations: the case where the inner tube of the heat exchanger is filled by the metal foam [41]; the case where the inner tube is surrounded by a metal foam [67]; and the case where the inner tube is filled and surrounded by metal foams [41,67]. The heat flux through the wall of the inner tube is assumed to be constant. Although the pressure drop correlation is arranged based on the heat exchanger tube’s diameter, the results indicate that the pressure drop is mainly a function of foam microstructure and it is caused by the foam solid structure rather than the pipe wall.

2.3. Category III: Metal foam channel heat exchangers

Kim et al. [43] established correlations for friction factor and overall heat transfer coefficient for metal foam channel heat exchangers via experimental techniques (Table 3, Eqs. (33)–(36)). The suggested friction factor equation is in good agreement with the correlation suggested by Beavers and Sparrow for the nickel foam metals [43,68]. In another work by Kim et al. [44], an empirical correlation for Nusselt number is established (Table 3, Eq. (37)). Lee and Vafai [61] developed an analytical solution for temperature distribution within a channel filled with a porous medium and subject to a constant heat flux boundary condition. They established an analytical relationship for Nusselt number as a function of solid and fluid effective thermal conductivities and solid–fluid interfacial characteristics utilizing local thermal nonequilibrium model (Table 3, Eqs. (38)–(40)). Marafie and Vafai [57] established analytical relationships for Nusselt number and temperature distribution for the channel subject to a constant heat flux utilizing Darcy–Forchheimer –Brinkman model and local thermal nonequilibrium model (Table 3, Eqs. (41) and (42)).

3. Performance evaluation of metal foam heat exchangers

Two types of counter flow metal foam heat exchangers are investigated to evaluate the efficiency improvement via inserting an aluminum foam in a heat exchanger. These are metal foam tube and channel heat exchangers. This is done by considering the generated heating and required pumping power to overcome the pressure drop. For the tube case, the inner tube is filled with the metal foam and for the channel case, the channel is filled with a metal foam. The working fluids are cold water and hot exhaust gas with properties of a mixture of 90% air and 10% CO<sub>2</sub>. Porosity, permeability, pore density and mean pore diameter of the foam matrix are taken as 0.9272,  $0.61 \times 10^{-7} \text{ m}^2$ , 23 PPI, and 0.00202 m, respectively. To evaluate friction factor, heat transfer coefficient and the overall heat transfer in the heat exchangers, Moody chart, pertinent correlations in the literature and the logarithmic mean temperature difference method were utilized [69].

3.1. Metal foam tube heat exchanger

The friction factor and required pumping power for two types of heat exchangers, with and without foam metal, are presented in Table 4 and the corresponding heat transfer coefficient and heat transfer rate for these heat exchangers are given in Table 5. Since the pressure drop is mainly affected by foam microstructure properties not the tube wall, changing the diameter of tube does not have a significant effect on the pressure drop. Note that increasing the velocity in both foam filled and plain tubes decreases the friction factor. The required pumping power is also presented in Table 4. Two pumping scenarios are considered here, an ideal efficiency case ( $\eta = 100\%$ ) and a low efficiency case ( $\eta = 30\%$ ).

Comparison of the heat transfer rates for the foam filled and the plain heat exchangers indicates a considerable increase in the heat transfer rate (8–13 times) when the metal foam is utilized (Table 5). An increase in flow rate (via velocity or tube diameter) will increase the heat transfer rate in both foam filled and plain heat exchang-

Table 4  
Friction factor and pressure drop of two types of metal foam heat exchangers compared to the plain heat exchangers

Case	Hot gas velocity (m/s)	Hot gas flow rate (m <sup>3</sup> /s)	Hot gas Reynolds number	Foam filled tube/channel				Plain tube/channel				Pressure drop ratio $\frac{(\Delta P/L)_{\text{Foam Filled}}}{(\Delta P/L)_{\text{Plain}}}$
				<i>f</i>	$\Delta P/L$ (Pa/m)	$\frac{P_{p,\eta=100\%}}{L}$ (W/m)	$\frac{P_{p,\eta=30\%}}{L}$ (W/m)	<i>f</i>	$\Delta P/L$ (Pa/m)	$\frac{P_{p,\eta=100\%}}{L}$ (W/m)	$\frac{P_{p,\eta=30\%}}{L}$ (W/m)	
Metal foam tube heat exchanger	5	$3.93 \times 10^{-4}$	2108	0.6373	5754	2.26	7.53	0.045	52.9	0.021	0.07	108.8
	10	$7.85 \times 10^{-4}$	4216	0.4287	15481	12.15	40.5	0.038	178.7	0.14	0.47	86.6
	10	$3.14 \times 10^{-3}$	8433	0.4287	15481	48.6	162	0.031	72.9	0.229	0.76	212.3
Metal foam channel heat exchanger	5	$3.93 \times 10^{-4}$	1869.7	4.13	10965.7	4.31	14.37	0.034	45.1	0.018	0.06	243.1

Table 5

Heat transfer coefficient, heat transfer rate and performance factor of two types of metal foam heat exchangers compared to the plain heat exchangers

Case	Hot gas velocity (m/s)	Hot gas flow rate (m <sup>3</sup> /s)	Hot gas Reynolds number	Foam filled tube/channel			Plain tube/channel			$\frac{(q/L)_{\text{Foam Filled}}}{(q/L)_{\text{Plain}}}$	Performance factor $\frac{(q-P_{p,\eta})_{\text{Foam Filled}} - (q-P_{p,\eta})_{\text{Plain}}}{(q-P_{p,\eta})_{\text{Plain}}} \times 100$	
				<i>Nu</i>	<i>h</i> (W/m <sup>2</sup> K)	q/L (W/m)	<i>Nu</i>	<i>h</i> (W/m <sup>2</sup> K)	q/L (W/m)		Ideal efficiency ( $\eta = 100\%$ )	Low efficiency ( $\eta = 30\%$ )
Metal foam tube heat exchanger	5	$3.93 \times 10^{-4}$	2108	700	2296	563	9.34	30.6	44.28	12.71	1167%	1156%
	10	$7.85 \times 10^{-4}$	4216	1400	4592	611.37	16.27	53.4	73.64	8.3	715%	680%
	10	$3.14 \times 10^{-3}$	8433	2100	3444	1014.15	28.33	46.46	127.6	7.95	658%	572%
Metal foam channel heat exchanger	5	$3.93 \times 10^{-4}$	1869.7	98.2	363.46	86.94	3.61	13.36	5.67	15.3	1362%	1193%

ers. Since flow rate may also increase the pressure drop, there is a need to also evaluate the net power. As such, a performance factor is introduced which represents the effects of both inserting metal foam in the heat exchanger and the losses due to the use of a pump. In Table 5, the net power is predicted based on the heat transfer rate and the required pumping power to overcome the pressure drop. As the table indicates the net power can increase by 1156% when inserting the metal foam even when utilizing a low efficiency pump ( $\eta = 30\%$ ). As such, microstructure properties of the foam metal, flow properties (flow rate, velocity, Reynolds number, ...) and tube/channel geometry should be taken into account to design an optimized heat exchanger.

### 3.2. Metal foam channel heat exchanger

The dimensions of the foam channel are taken in a way to result in the same flow rate as the tube heat exchanger. As expected, there is an increase in the pressure drop when inserting the metal foam (Table 4). As seen in Table 5, the heat transfer rate is enhanced by more than 15 times and the performance factor which represents the net produced power increases by more than 1100% by inserting the metal foam.

## 4. Conclusions

Metal foam heat exchangers have substantial advantages compared to commercially available heat exchangers under nearly identical conditions. They provide substantially more heat transfer surface area, and more boundary layer disruption and mixing resulting from foam filaments. This leads to considerably larger heat transfer rates. Metal foam microstructural properties, such as pore size, pore density, relative density, and porosity, control the heat transfer processes. Decreasing the pore size or porosity or increasing the relative density or pore density results in higher heat transfer and pressure drop. For a specific application, a compromise between the heat transfer rate and pressure drop should be employed. Metal foams are classi-

fied as highly porous and tortuous materials. For many foam metal applications, it is best to employ the local thermal nonequilibrium (LTNE) form of the energy equation. For the LTNE model, the solid-to-fluid heat transfer coefficient can be estimated based on modified correlations for flow over a cylinder. In this work, the pertinent models for flow and thermal transport through metal foam heat exchangers were categorized and discussed in some detail. Two prominent types of heat exchangers, namely, the tube and channel heat exchangers were investigated to evaluate the effect of metal foams on heat exchanger performance. The results indicate a considerable improvement in performance by inserting the metal foam. The effect of this increase on the pressure was also investigated. It was found that even a low efficiency pump might be enough to overcome the additional pressure drop.

## References

- [1] L. Tianjian, Ultralight porous metals: from fundamentals to applications, *Acta Mechanica Sinica, Chinese J. Mech.* 18 (5) (2002) 457–479.
- [2] B. Alazmi, K. Vafai, Analysis of fluid flow and heat transfer interfacial conditions between a porous medium and a fluid layer, *Int. J. Heat Mass Transfer* 44 (2001) 1735–1749.
- [3] A. Amiri, K. Vafai, T.M. Kuzay, Effect of boundary conditions on non-Darcian heat transfer through porous media and experimental comparisons, *Numer. Heat Transfer J.* 27 Part A (1995) 651–664.
- [4] M.L. Hunt, C.L. Tien, Effects of thermal dispersion on forced convection in fibrous media, *Int. J. Heat Mass Transfer* 31 (2) (1988) 301–309.
- [5] A. Amiri, K. Vafai, Analysis of dispersion effects and non-thermal equilibrium non-Darcian, variable porosity incompressible flow through porous medium, *Int. J. Heat Mass Transfer* 37 (1994) 939–954.
- [6] C.Y. Zhao, T. Kim, T.J. Lu, H.P. Hodson, Thermal transport in high porosity cellular metal foams, *J. Thermophys. Heat Transfer* 18 (3) (2004) 309–317.
- [7] K. Vafai, C.L. Tien, Boundary and inertia effects on convective mass transfer in porous media, *Int. J. Heat Mass Transfer* 25 (8) (1982) 1183–1190.
- [8] C.R. Edmundo, Modeling of heat transfer in open cell metal foams, Master Thesis, University of Puerto Rico, 2004.
- [9] K. Vafai, A. Amiri, Non-Darcian effects in confined forced convective flows, *Transport Phenomena in Porous Media, Elsevier Science* (1998) 313–329.

- [10] M. Sozen, K. Vafai, Longitudinal heat dispersion in packed beds with real gas flow, *AIAA J. Thermophys. Heat Transfer* 7 (1993) 153–157.
- [11] K. Vafai, A. Bejan, W.J. Minkowycz, K. Khanafer, A critical synthesis of pertinent models for turbulent transport through porous media, *handbook of numerical heat transfer*, 2nd ed., John Wiley and Sons Inc., New Jersey, 2006, pp. 389–416.
- [12] B. Alazmi, K. Vafai, Analysis of variable porosity, thermal dispersion, and local thermal nonequilibrium on free surface flows through porous media, *ASME J. Heat Transfer* 126 (2004) 389–399.
- [13] D.P. Haack, K.R. Butcher, T. Kim, T.J. Lu, Novel lightweight metal foam heat exchangers, *Porvair Fuel Cell Technology, Inc., USA*, 2001.
- [14] W.E. Azzi, A systematic study on the mechanical and thermal properties of open cell metal foams for aerospace applications, Master Thesis, North Carolina State University, 2004.
- [15] M.A. Janney, Overview of fuel cell activities at PFCT, *Porvair Fuel Cell Technology, Inc., USA*, 2005.
- [16] S. Sharafat, M. Demetriou, N. Ghoniem, B. Williams, R. Nygren, Enhanced surface heat removal using a porous Tungsten heat exchanger, *Am. Nucl. Soc. Topical Meeting Technol. Fusion Energy* 39 (2) (2001) 863–867.
- [17] T.J. Lu, H.A. Stone, M.F. Ashby, Heat transfer in open cell metal foams, *Acta Mater.* 46 (10) (1998) 3619–3635.
- [18] K. Boomsma, D. Poulikakos, F. Zwick, Metal foams as compact high performance heat exchangers, *J. Mech. Mater.* 35 (2003) 1161–1176.
- [19] S. Ebara, S. Toda, H. Hashizume, Application of porous matrix to high heat load removal system, *Heat Mass Transfer* 36 (2000) 273–276.
- [20] D.A. Zumbrunnen, R. Viskanta, F.P. Incropera, Heat transfer through porous solids with internal geometries, *Int. J. Heat Mass Transfer* 29 (1986) 275–284.
- [21] A.F. Bastawros, Effectiveness of open-cell metallic foams for high power electronic cooling, *Proceeding Symposium on the Thermal Management of Electronics*, IMECE Anaheim, CA, 1998.
- [22] R. Rachedi, S. Chikh, Enhancement of electronic cooling by insertion of foam materials, *Heat Mass Transfer* 37 (2001) 371–378.
- [23] B.V. Antohe, J.L. Lage, D.C. Price, R.M. Weber, Numerical characterization of micro heat exchangers using experimentally tested porous aluminum layers, *Int. J. Heat Fluid Flow* 17 (6) (1996) 594–603.
- [24] A. Bhattacharya, R.L. Mahajan, Finned metal foam heat sinks for electronics cooling in forced convection, *J. Elect. Packag.* (124) (2002) 155–163.
- [25] P.D. Dunn, D.A. Reay, The heat pipe, *Phys. Technol.* 4 (1973) 187–201.
- [26] Y. Wang, K. Vafai, An experimental investigation of the thermal performance of an asymmetrical flat plate heat pipe, *Int. J. Heat Mass Transfer* 43 (2000) 2657–2668.
- [27] T.J. Lu, A. Hess, M.F. Ashby, Sound absorption in metallic foams, *J. Appl. Phys.* 85 (11) (1999) 7528–7539.
- [28] M.E. Delany, E.N. Bazley, Acoustical properties of fibrous absorbent materials, *Appl. Acoust.* 3 (1) (1969) 105–116.
- [29] J.F. Allard, Y. Champoux, New empirical equations for sound propagation in rigid frame fibrous materials, *J. Acoust. Soc. Am.* 91 (6) (1992) 3346–3353.
- [30] K. Attenborough, Acoustical characteristics of rigid fibrous absorbents and granular materials, *J. Acoust. Soc. Am.* 73 (3) (1983) 785–799.
- [31] J.F. Liu, W.T. Wu, W.C. Chiu, W.H. Hsieh, Measurement and correlation of friction characteristic of flow through foam matrixes, *Exp. Thermal Fluid Sci.* 30 (2006) 329–336.
- [32] N. Dukhan, Correlations for the pressure drop for flow through metal foam, *Exp. Fluids* 41 (2006) 665–672.
- [33] K. Boomsma, D. Poulikakos, Y. Ventikos, Simulations of flow through open cell metal foams using an idealized periodic cell structure, *Int. J. Heat Fluid Flow* 24 (2003) 825–834.
- [34] B. Alazmi, K. Vafai, Analysis of variants within the porous media transport models, *ASME J. Heat Transfer* 122 (2000) 303–326.
- [35] Q. Yu, A.G. Straatman, B.E. Thompson, Carbon-foam finned tubes in air–water heat exchangers, *J. Appl. Thermal Eng.* 26 (2006) 131–143.
- [36] V.V. Calmidi, R.L. Mahajan, Forced convection in high porosity metal foams, *ASME J. Heat Transfer* 122 (2000) 557–565.
- [37] P. Du Plessis, A. Montillet, J. Comiti, J. Legrand, Pressure drop prediction for flow through high porosity metallic foams, *Chem. Eng. Sci.* 49 (21) (1994) 3545–3553.
- [38] J.G. Fourie, J.P. Du Plessis, Pressure drop modelling in cellular metallic foams, *Chem. Eng. Sci.* 57 (2002) 2781–2789.
- [39] V.V. Calmidi, Transport phenomena in high porosity metal foams, PhD. Thesis, University of Colorado, 1998.
- [40] A. Bhattacharya, V.V. Calmidi, R.L. Mahajan, Thermophysical properties of high porosity metal foams, *Int. J. Heat Mass Transfer* 45 (2002) 1017–1031.
- [41] W. Lu, C.Y. Zhao, S.A. Tassou, Thermal analysis on metal foam filled heat exchangers Part I: Metal-foam filled pipes, *Int. J. Heat Mass Transfer* 49 (2006) 2751–2761.
- [42] J. Klett, D. Stinton, R. Ott, C. Walls, R. Smith, B. Conway, Heat exchangers/radiators utilizing graphite foams, *Oak Ridge National Laboratory, US Department of Energy*, 2001.
- [43] S.Y. Kim, J.W. Paek, B.H. Kang, Flow and heat transfer correlations for porous fin in a plate-fin heat exchanger, *ASME J. Heat Transfer* 122 (2000) 572–578.
- [44] S.Y. Kim, B.H. Kang, J.H. Kim, Forced convection from aluminum foam materials in an asymmetrically heated channel, *Int. J. Heat Mass Transfer* 44 (2001) 1451–1454.
- [45] V.V. Calmidi, R.L. Mahajan, The effective thermal conductivity of high porosity fibrous metal foams, *ASME J. Heat Transfer* 121 (1999) 466–471.
- [46] T.J. Lu, C. Chen, Thermal transport and fire retardance properties of cellular aluminum alloys, *ACTA Mater.* 47 (5) (1999) 1469–1485.
- [47] J.W. Paek, B.H. Kang, S.Y. Kim, J.M. Hyun, Effective thermal conductivity and permeability of aluminum foam materials, *Int. J. Thermophys.* 21 (2) (2000) 453–464.
- [48] M.K. Alam, B. Maruyama, Thermal conductivity of graphitic carbon foams, *Exp. Heat Transfer* 17 (2004) 227–241.
- [49] C.Y. Zhao, T.J. Lu, H.P. Hodson, J.D. Jackson, The temperature dependence of effective thermal conductivity of open-celled steel alloy foams, *Mater. Sci. Eng. A* 367 (1–2) (2004) 123–131.
- [50] R. Singh, H.S. Kasana, Computational aspects of effective thermal conductivity of highly porous metal foams, *Appl. Thermal Eng.* 24 (13) (2004) 1841–1849.
- [51] J.G. Fourie, J.P. Du Plessis, Effective and coupled thermal conductivities of isotropic open cellular foams, *AIChE J.* 50 (3) (2004) 547–556.
- [52] N. Dukhan, R. Picon-Feliciano, A.R. Alvarez-Hernandez, Heat transfer analysis in metal foams with low conductivity fluids, *J. Heat Transfer* 128 (2006) 784–792.
- [53] D.L. Koch, J.F. Brady, The effective diffusivity of fibrous media, *AIChE J.* 32 (4) (1986) 575–591.
- [54] K. Boomsma, D. Poulikakos, On the effective thermal conductivity of a three-dimensionally structured fluid-saturated metal foam, *Int. J. Heat Mass Transfer* 44 (2001) 827–836.
- [55] N. Dukhan P. Quinones, Convective heat transfer analysis of open cell metal foam for solar air heaters, *Proceeding of International Solar Energy Conference USA*, 2003.
- [56] M.S. Phanikumar, R.L. Mahajan, Non-Darcy natural convection in high porosity metal foams, *Int. J. Heat Mass Transfer* 45 (2002) 3781–3793.
- [57] A. Marafie, K. Vafai, Analysis of non-Darcian effects on temperature differentials in porous media, *Int. J. Heat Mass Transfer* 44 (2001) 4401–4411.
- [58] A. Amiri, K. Vafai, Analysis of dispersion effects and nonthermal equilibrium, non-Darcian, variable porosity incompressible flow

- through porous medium, *Int. J. Heat Mass Transfer* 37 (1994) 939–954.
- [59] A. Amiri, K. Vafai, Transient analysis of incompressible flow through a packed bed, *Int. J. Heat Mass Transfer* 41 (1998) 4259–4279.
- [60] B. Alazmi, K. Vafai, Constant wall heat flux boundary conditions in porous media under local thermal non-equilibrium conditions, *Int. J. Heat Mass Transfer* 45 (2002) 3071–3087.
- [61] D.Y. Lee, K. Vafai, Analytical characterization and conceptual assessment of solid and fluid temperature differentials in porous media, *Int. J. Heat Mass Transfer* 42 (1999) 423–435.
- [62] S. Ergun, Fluid flow through packed columns, *Chem. Eng. Prog.* 48 (1952) 89–94.
- [63] B.V. Antohe, J.L. Lage, D.C. Price, R.M. Weber, Experimental determination of the permeability and inertial coefficients of mechanically compressed aluminum porous matrices, *ASME J. Fluids Eng.* 119 (1997) 404–412.
- [64] L. Tadrif, M. Miscevic, O. Rahli, F. Topin, About the use of fibrous materials in compact heat exchangers, *Exp. Thermal Fluid Sci.* 28 (2–3) (2004) 193–199.
- [65] W.H. Shih, W.C. Chiu, W.H. Hsieh, Height effect on heat transfer characteristics of aluminum foam heat sinks, *J. Heat Transfer* 128 (2006) 530–537.
- [66] A. Zukauskas, Convective heat transfer in cross-flow, in: S. Kakas, R.K. Shah, W. Aung (Eds.), *Handbook of single-phase convective heat transfer*, Wiley, New York, 1987.
- [67] C.Y. Zhao, W. Lu, S.A. Tassou, Thermal analysis on metal-foam filled heat exchangers. Part II: Tube heat exchangers, *Int. J. Heat Mass Transfer* 49 (2006) 2762–2770.
- [68] G.S. Beavers, E.M. Sparrow, Non-Darcy flow through fibrous porous media, *J. Appl. Mech.* 36 (1969) 711–714.
- [69] F.P. Incropera, D.P. Dewitt, *Fundamentals of heat and mass transfer*, Wiley, 2002.